# Divergent Reactivity of a Phosphinidene-Bridged Dimolybdenum Complex Toward 1-Alkynes: P–C, P–H, C–C, and C–H Couplings

M. Esther García, Daniel García-Vivó,* Miguel A. Ruiz,* and David Sáez

Departamento de Química Orgánica e Inorgánica / IUQOEM, Universidad de Oviedo, E-33071 Oviedo, Spain.

*Supporting Information Placeholder*

**ABSTRACT:** The ability of complex $[Mo_2Cp_2\{\mu\text{-}P(2,4,6\text{-}C_6H_2{}^tBu_3)\}(CO)_4]$ to promote P–C and subsequent coupling processes has been analyzed by examining reactions with alkynes. The title compound reacted at room temperature with different terminal alkynes HC≡CR under visible-UV light irradiation to give, in a selective way, the corresponding phosphapropenediyl derivatives $[Mo_2Cp_2(\mu\text{-}\kappa^1_C{:}\eta^3_{C,C,P}\text{-}CRCHPR^*)(CO)_4]$ for R groups of varied electron-withdrawing nature, but low to medium size, such as Pr, $CO_2Me$, and *p*-tol. These products follow from formal insertion of the alkyne into one of the Mo-phosphinidene bonds in the parent compound, with selective P–C coupling to the terminal carbon of the alkyne. In contrast, when R was the bulky $^t$Bu group, the corresponding photochemical reactions yielded a mixture of the *cis* and *trans* isomers of the phosphanyl- and formylalkenyl-bridged complex $[Mo_2Cp_2\{\mu\text{-}\kappa^2_{C,O}{:}\eta^2_{C,C}\text{-}CHC(^tBu)C(O)H\}\{\mu\text{-}P(CH_2CMe_2)C_6H_2{}^tBu_2\}(CO)_2]$, which follow from a complex reaction sequence involving an H–C($sp^3$) bond cleavage along with different P–C, P–H, C–C and C–H bond formation steps. Density functional theory calculations were carried out to rationalize the preceding observations, and suggested that an isomer of the parent complex displaying a bent terminal phosphinidene ligand might be involved in all the above photochemical reactions.

## INTRODUCTION

Phosphinidene complexes, like other species bearing a low-coordinated P atom, are very reactive species with a significant use as precursors of new organophosphorus derivatives *via* reactions with different organic molecules.[1] When reacting with alkynes, these complexes are expected to undergo P–C coupling, although the final product will be strongly dependent on the particular nature of the metal complex under study. Electrophilic mononuclear complexes having bent terminal ligands usually undergo [1+2] cycloaddition to yield phosphirene derivatives,[2] whereas their nucleophilic counterparts rather undergo [2+2] cycloaddition to yield products displaying metallaphosphacyclobutene rings.[3]

**Chart 1**

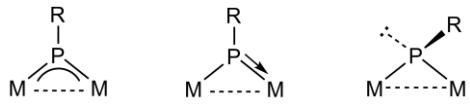


Binuclear complexes having bridging phosphinidene ligands react with alkynes in more complex ways, in turn depending on the particular coordination mode of the phosphinidene ligand (**A** to **C** in Chart 1).[4] This is particularly well illustrated by the type **C** diiron complex $[Fe_2Cp_2(\mu\text{-}PCy)(\mu\text{-}CO)(CO)_2]$, which reacts with alkynes to give a large variety of products depending on the particular alkyne and reactions conditions (cf. Scheme 1), although they all seem to follow from a common zwitterionic intermediate formed upon initial nucleophilic attack of the pyramidal phosphinidene ligand to the less protected carbon of the alkyne.[5] This sort of reactivity also seems to be under operation in the reactions of the type **B** dimolybdenum complexes $[Mo_2Cp_2(\mu\text{-}PH)(CO)_2(\eta^6\text{-}R^*H)]$ and $[Mo_2Cp(\mu\text{-}\kappa^1{:}\kappa^1,\eta^5\text{-}PC_5H_4)(\eta^6\text{-}R^*H)(CO)_2]$ with alkynes (Cp = $\eta^5$-$C_5H_5$; R* = 2,4,6-$C_6H_2{}^tBu_3$), which may eventually yield products of formal [2+2] cycloaddition of the alkyne to the Mo–P double bond of these substrates (cf. Scheme 2).[6]

**Scheme 1. Reactions of Phosphinidene Complexes of type C with Alkynes[5]**

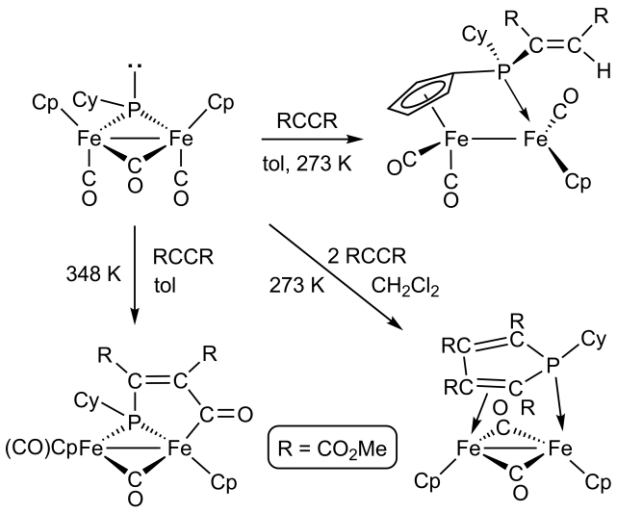


As for trigonal phosphinidene complexes of type **A**, early work by Huttner revealed a cycloaddition-like behavior of the transient (and electron deficient) complex $[Fe_2(\mu\text{-}P^tBu)(CO)_6]$

when faced with different alkynes (Scheme 3).[7] In contrast, in a preliminary study on the chemistry of the electron-precise dimolybdenum complex $[Mo_2Cp_2(\mu\text{-PR*})(CO)_4]$ (**1**) we found that its photochemical reaction with HC≡C(*p*-tol) resulted in full and selective insertion of the alkyne into one of the Mo–P bonds to yield a rare phosphapropenediyl complex $[Mo_2Cp_2\{\mu\text{-}\kappa^1_C\text{:}\eta^3_{C,C,P}\text{-C(}p\text{-tol)CHPR*}\}(CO)_4]$ (**2-tol**).[8] Note the reversed selectivity of the P–C couplings in the $Fe_2$ and $Mo_2$ substrates (Scheme 3). The presence of a lone pair at the P atom in **2-tol** was surprising and led us to postulate the participation in this reaction of a tautomer of **1** having a pyramidal phosphinidene ligand of type **C**. Puzzled by this singular behavior of compound **1** we decided to further explore its photochemical reactivity toward alkynes, which is the purpose of the present work. As shown below, steric effects play a critical role in these reactions. We have also examined computationally the role of likely isomers of **1** which might display enhanced reactivity toward alkynes and thus better explain the results of these multistep reactions, and concluded that an isomer of **1** having a bent terminal phosphinidene ligand is likely responsible for all products formed, *via* two different reaction pathways.

**Scheme 2. Reactions of Phosphinidene Complexes of type B with Alkynes[6]**

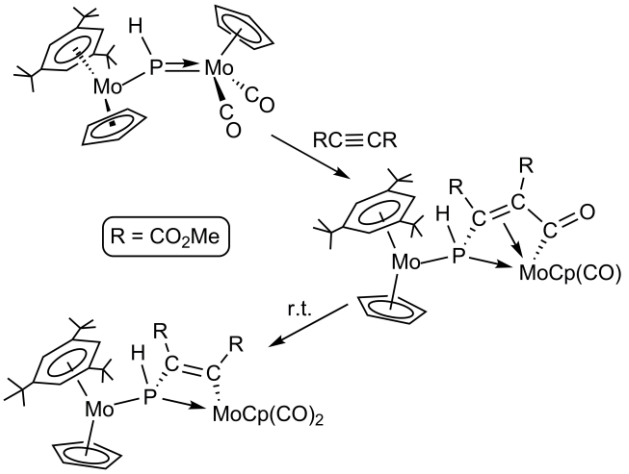


**Scheme 3. Reactions of Phosphinidene Complexes of type A with Alkynes[7,8]**

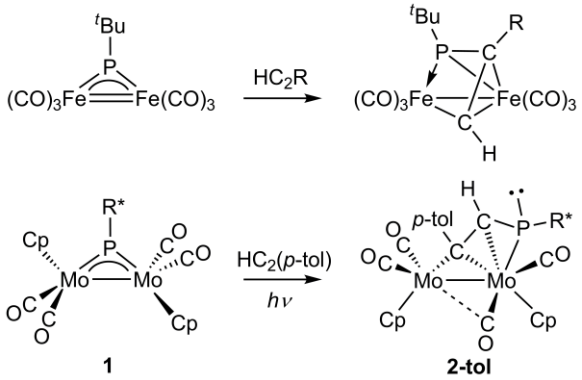


## RESULTS AND DISCUSSION

**Photochemical Reactions of Complex 1 with 1-Alkynes**. Compound **1** did not react with internal alkynes such as diphenylacetylene or 3-hexyne under photochemical conditions. In contrast, reactions of **1** with different terminal alkynes HC≡CR proceeded readily at room temperature under irradiation with visible-UV light, although the product was very sensitive to the size of the substituent R. Thus, for R groups of varied electron-withdrawing nature but low to moderate size, such as Pr, $CO_2Me$ and *p*-tol, the corresponding phosphapropenediyl derivatives $[Mo_2Cp_2(\mu\text{-}\kappa^1_C\text{:}\eta^3_{C,C,P}\text{-CRCHPR*})(CO)_4]$ (**2-R**) were obtained in a selective way, with specific formation of a P–C bond between the phosphinidene ligand and the terminal carbon of the alkyne (Chart 2). In contrast, when R was the bulky $^t$Bu group, the corresponding photochemical reactions yielded no derivatives of type **2**, but a mixture of the *cis* and *trans* isomers of the phosphanyl complex $[Mo_2Cp_2\{\mu\text{-}\kappa^2_{C,O}\text{:}\eta^2_{C,C}\text{-CHC(}^t\text{Bu)C(O)H}\}\{\mu\text{-P(CH}_2\text{CMe}_2\text{)C}_6\text{H}_2{}^t\text{Bu}_2\}(CO)_2]$ (***cis*-3** and ***trans*-3**), which additionally display a bridging formylalkenyl ligand (Chart 2). The radiation wavelength had a significant influence on the ratio of isomers formed, with the *cis* isomer being formed preferentially when using the more transparent quartz glassware, whereas the use of Pyrex glassware (which filters off much of the most energetic UV radiation) led to a mixture having the *trans* isomer as the major product. Separate experiments revealed that these isomers did not interconvert under the above photochemical conditions, this indicating that their formation occurs *via* independent reaction pathways.

**Chart 2**

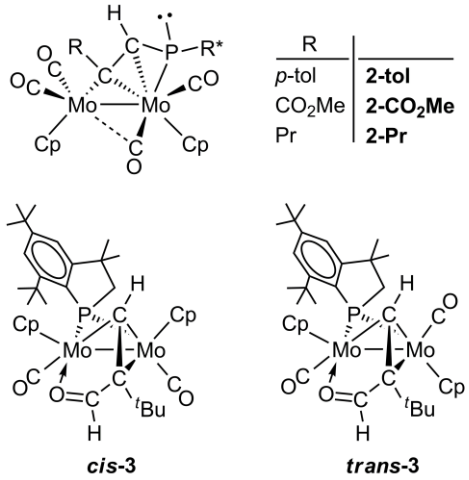


The formation of the phosphanyl complexes **3** requires a complex combination of elemental steps involving, *inter alia*, a C–H bond cleavage in a $^t$Bu group. Interestingly, we recall that photolysis of **1** in toluene solution induces itself a C–H cleavage of a $^t$Bu group, eventually yielding its isomeric hydride complex $[Mo_2Cp_2(\mu\text{-H})\{\mu\text{-P(CH}_2\text{CMe}_2\text{)C}_6\text{H}_2{}^t\text{Bu}_2\}(CO)_4]$ (**4**) (Scheme 4),[8,9] with a bridging phosphanyl ligand identical to the one found in complexes **3**. We then checked a possible involvement of the hydride **4** in the formation of complexes **3**, and found that no detectable amounts of these compounds were formed when irradiating mixtures of **4** and HC≡C$^t$Bu under analogous conditions.

**Scheme 4. Photochemical Isomerization of Compound 1[8,9]**

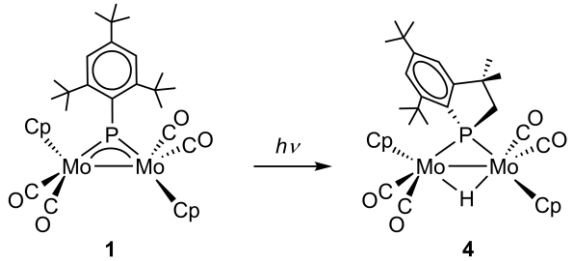

**Structural Characterization of Phosphapropenediyl Complexes 2**. The structure of compound **2-tol** (Figure 1) was determined by an X-ray study during our preliminary analysis of the chemistry of **1**,[8] but it was not discussed at the time. Since this complex remains a unique example of a four-electron-donor bridging phosphapropenediyl (CRCRPR) ligand, a brief discussion on the matter has to be done. Actually only a few complexes having this sort of ligand have been structurally characterized so far, most of them also made through insertion of alkynes into the M–P bond of suitable phosphinidene-bridged complexes. With the exception of the diiron complex depicted in Scheme 3, which displays a six-electron donor bridging ligand of type $\mu_2$-*C*,*P*:*C*,*C*,*P*, all other structurally characterized examples correspond to tri- and tetranuclear species (most of them Fe or Ru clusters) displaying six-electron donor ligands of the types $\mu_3$-*C*:*C*,*C*,*P*:*P* and $\mu_4$-*C*:*C*,*C*,*P*:*P*:*P*, respectively.[10,11]

The molecule of **2-tol** is built from two $MoCp(CO)_2$ fragments connected *via* an intermetallic bond (3.1573(5) Å) and the four-electron-donor bridging RCCHPR* ligand. The latter might be viewed as $\sigma$-bound to Mo1 *via* the bridgehead C30 atom (Mo1–C30 = 2.179(3) Å), and $\pi$-bound to Mo2 in an allyl-like fashion, *via* the C30, C29 and P atoms (Mo2–C ca. 2.28 Å, Mo2–P = 2.6646(7) Å). As a result, the C29–C30 separation of ca. 1.42 Å expectedly falls between the reference distances for single and double C–C bonds, and is comparable to the values measured in the mentioned examples having six-electron-donor CRCRPR ligands (range 1.36-1.45 Å). Interestingly, the P–C29 length of 1.761(3) falls in turn between the reference values for P–C($sp^2$) single and double bonds (1.80 and 1.66 Å, respectively),[12,13] a circumstance which suggests that the lone electron pair at the P atom might be involved at some extent in $\pi$-bonding with the C29 atom, even if the P environment actually is pyramidal ($\Sigma$X–P–Y ca. 262°). Over all, this molecule is a 34-electron complex, for which a single intermetallic bond must be formulated according to the 18-electron rule, which is in agreement with the relatively large intermetallic separation of ca. 3.15 Å (cf. 3.220(3) Å in the parent compound **1**).[14] We finally note that the intrinsic asymmetry of the bridging phosphapropenediyl ligand, which formally contributes with one electron to Mo1 and three electrons to the Mo2 atom, is partially balanced by the C4O4 carbonyl, with geometric parameters characteristic of a bent semibridging ligand (Mo–C lengths ca. 2.01 and 2.55 Å, Mo2–C4–O4 ca. 154°, asymmetry parameter $\alpha$ = 0.27).[15]

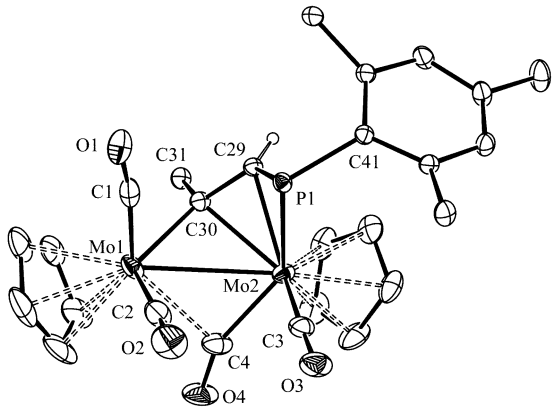


**Figure 1**. ORTEP drawing (30% probability) of compound **2-tol**, with *p*-tolyl and $^t$Bu groups (except their $C^1$ atoms), and most H atoms omitted for clarity.[8] Selected bond lengths (Å) and angles (°): Mo1–Mo2 = 3.1573(5), Mo1–C30 = 2.179(3), Mo1–C4 = 2.551(4), Mo2–C4 = 2.012(3), Mo2–C3 = 1.981(3), Mo2–P1 = 2.6646(7), Mo2–C29 = 2.285(3), Mo2–C30 = 2.284(3), P1–C29 = 1.761(3), P1–C41 = 1.866(2), C29–C30 = 1.423(3); Mo2–C4–O4 = 154.0(3), P1–C29–C30 = 122.4(2).

**Table 1. Selected IR and NMR Data for New Compounds**

| Compound | $\nu$(CO)[a] | $\delta$(P)[b] |
|---|---|---|
| $[Mo_2Cp_2(\mu\text{-PR*})(CO)_4]$ (**1**)[c] | 1958 (w, sh), 1921 (vs), 1880 (s), 1856 (s) | 685.6 |
| $[Mo_2Cp_2\{\mu\text{-}\kappa^1_C\text{:}\eta^3_{C,C,P}\text{-C}(p\text{-tol})CHPR^*\}(CO)_4]$ (**2-tol**) | 1959 (vs), 1915 (s), 1848 (m), 1806 (w) | 18.0 |
| $[Mo_2Cp_2\{\mu\text{-}\kappa^1_C\text{:}\eta^3_{C,C,P}\text{-C}(CO_2Me)CHPR^*\}(CO)_4]$ (**2-CO$_2$Me**) | 1967 (vs), 1920 (s), 1861 (m), 1811 (w)[d] | 23.0 |
| $[Mo_2Cp_2\{\mu\text{-}\kappa^1_C\text{:}\eta^3_{C,C,P}\text{-C(Pr)}CHPR^*\}(CO)_4]$ (**2-Pr**) | 1950 (vs), 1911 (s), 1850 (m), 1794 (w) | 21.0 |
| *cis*-$[Mo_2Cp_2\{\mu\text{-}\kappa^2_{C,O}\text{:}\eta^2_{C,C}\text{-CHC}(^t\text{Bu})C(O)H\}\{\mu\text{-}P(CH_2CMe_2)C_6H_2{}^t\text{Bu}_2\}(CO)_2]$ (***cis*-3**) | 1949 (vs), 1837 (m) | 164.9 |
| *trans*-$[Mo_2Cp_2\{\mu\text{-}\kappa^2_{C,O}\text{:}\eta^2_{C,C}\text{-CHC}(^t\text{Bu})C(O)H\}\{\mu\text{-}P(CH_2CMe_2)C_6H_2{}^t\text{Bu}_2\}(CO)_2]$ (***trans*-3**) | 1969 (s), 1810 (vs) | 141.4 |
| $[Mo_2Cp_2(\mu\text{-H})\{\mu\text{-}P(CH_2CMe_2)C_6H_2{}^t\text{Bu}_2\}(CO)_4]$ (**4**)[c] | 1958 (w, sh), 1936 (vs), 1862 (s) | 166.8 |

[a] Recorded in dichloromethane solution, $\nu$ in $cm^{-1}$. [b] Recorded in $CD_2Cl_2$ solutions at 290 K and 121.50 MHz; $\delta$ in ppm relative to external 85% aqueous $H_3PO_4$. [c] Data taken from reference 9. [d] $\nu$(CO) ($CO_2Me$) = 1677 (w).

Spectroscopic data in solution for compounds **2** (Table 1 and Experimental Section) are in agreement with the structure found in the crystal for **2-tol**. The IR spectrum of these compounds display in each case four C–O stretches for the carbonyl ligands, with the one at higher frequency being also the most intense one, in agreement with the cisoid arrangement of the binuclear $[M(CO)_2]_2$ oscillator of these molecules.[16] We also note that the less energetic band appears at a significantly low frequency of ca. 1800 $cm^{-1}$, consistent with the presence of a semibridging carbonyl, while the average frequency for

all C–O stretches correlates well with the electron-releasing properties of the R substituent, since it increases in the order **2-Pr** < **2-tol** < **2-$CO_2$Me** as expected.

Compounds **2** display a $^{31}$P NMR resonance at ca. 20 ppm, dramatically shielded by some 660 ppm with respect to the parent compound **1**. This low chemical shift indicates that the pyramidal, phosphanyl-like environment found for the P atom in the solid state, is preserved in solution (cf. $\delta_P$ –31.9 ppm for [MoCp($PPh_2$)($CO)_2$($PMe_3$)]).[17] As for the NMR spectra, we note that the central CH group of the bridging *C,C,P*-donor ligand in compounds **2** gives rise to characteristic resonances at ca. 6 ppm ($^1$H) and 115 ppm ($^{13}$C), the latter being strongly coupled to P as expected ($^1J_{PC}$ ca. 60 Hz), with little influence of the substituent R. In contrast, the bridgehead carbon atom gives rise to a more deshielded resonance, with a chemical shift quite sensitive to the R substituent bound to it [$\delta_C$ 151.4 ($CO_2$Me), 179.1 (*p*-tol), 197.4 (Pr)]. We finally note that these compounds display in each case four distinct carbonyl resonances as expected. Compounds **2-tol** and **2-$CO_2$Me** display a strongly deshielded carbonyl resonance at ca. 254 ppm, almost 20 ppm above the less deshielded resonance (ca. 234 ppm), which can be assigned to the semibridging ligand present in the solid state. In contrast, compound **2-Pr** displays two resonances at ca. 249 ppm and two other at ca. 240 ppm, which might be indicative of the presence of two, rather than one, semibridging carbonyls in this complex.

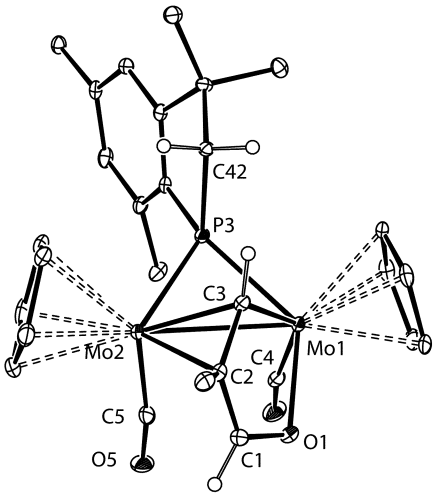


**Figure 2**. ORTEP drawing (30% probability) of ***cis*-3**, with $^t$Bu groups (except their C$^1$ atoms), and most H atoms omitted.

**Structural Characterization of the Phosphanyl Complexes *cis*-3 and *trans*-3.** The structures of these isomers in the crystal are shown in Figures 2 and 3, while the relevant geometrical parameters are collected in Tables 2 and 3. Both molecules are built from two MoCp(CO) fragments bridged by a phosphanyl ligand derived from intramolecular cyclization at the former phosphinidene ligand, following from a H–C($^t$Bu) bond cleavage analogous to the one observed in the formation of the hydride complex **4**. The second bridging group, however, is a formylalkenyl ligand resulting from coupling of the added alkyne, a carbonyl ligand and the H atom of the degraded $^t$Bu group. This ligand can be viewed as $\sigma$-bound to one of the metal atoms (Mo1) *via* the bridgehead alkenyl carbon and the oxygen atom of the formyl group, and $\pi$-bound to the second metal atom (Mo2) *via* the alkenyl C–C double bond.

**Table 2. Selected Bond Lengths (Å) and Angles (º) for Compound *cis*-3.**

| | | | |
|---|---|---|---|
| Mo1–Mo2 | 3.0047(5) | Mo2–Mo1–C4 | 91.6(1) |
| Mo1–P | 2.440(1) | Mo1–Mo2–C5 | 78.9(1) |
| Mo2–P | 2.455(1) | C4–Mo1–P | 93.4(1) |
| Mo1–C4 | 1.996(3) | C5–Mo2–P | 102.6(1) |
| Mo2–C5 | 1.951(3) | C3–Mo1–P | 72.4(1) |
| Mo1–C3 | 2.142(3) | C3–Mo2–P | 71.5(1) |
| Mo1–O1 | 2.147(2) | C2–Mo2–P | 107.5(1) |
| Mo2–C3 | 2.175(3) | O1–Mo1–P | 128.4(1) |
| Mo2–C2 | 2.343(3) | | |
| C3–C2 | 1.430(4) | | |
| C1–O1 | 1.292(3) | | |

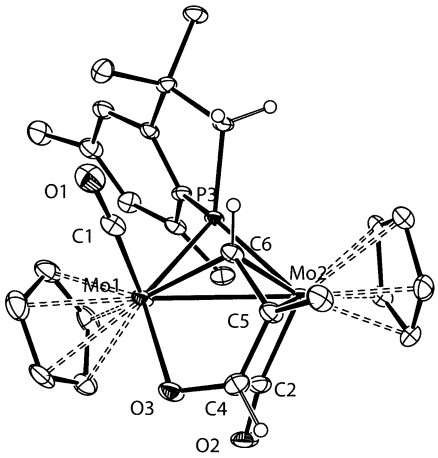


**Figure 3**. ORTEP drawing (30% probability) of ***trans*-3**, with $^t$Bu groups (except their C$^1$ atoms), and most H atoms omitted.

**Table 3. Selected Bond Lengths (Å) and Angles (º) for Compound *trans*-3.**

| | | | |
|---|---|---|---|
| Mo1–Mo2 | 2.959(3) | Mo2–Mo1–C1 | 109.7(2) |
| Mo1–P | 2.468(2) | Mo1–Mo2–C2 | 69.5(2) |
| Mo2–P | 2.407(2) | C1–Mo1–P | 95.6(2) |
| Mo1–C1 | 1.905(7) | C2–Mo2–P | 98.3(2) |
| Mo2–C2 | 1.929(6) | C6–Mo1–P | 69.9(1) |
| Mo1–C6 | 2.166(6) | C6–Mo2–P | 71.5(2) |
| Mo1–O3 | 2.141(4) | C5–Mo2–P | 108.0(2) |
| Mo2–C6 | 2.145(6) | O3–Mo1–P | 132.0(1) |
| Mo2–C5 | 2.364(6) | | |
| C6–C5 | 1.455(7) | | |
| C4–O3 | 1.282(8) | | |

The geometrical parameters within the bridging ligands for both isomers are similar to each other, and the most significant

difference of course is the relative arrangement of the terminal Cp and CO ligands, which is of the cisoid type for ***cis*-3** (Mo–Mo–CO angles ca. 80-90°), and of the distorted transoid type for ***trans*-3**, with one carbonyl leaning over the intermetallic bond and the other one pointing away from the dimetal center (Mo–Mo–CO angles ca. 70 and 110° respectively). Overall, the structures of these isomers are very similar to those of the *cis* and *trans* isomers of the alkenyl complex $[Mo_2Cp_2(\mu\text{-}\kappa^2_{C,O}\text{:}\eta^2_{C,C}\text{-CRCHR})(\mu\text{-}PCy_2)(CO)_2]$ (R = $CO_2Me$), a molecule formed in the reaction of the unsaturated hydride $[Mo_2Cp_2(\mu\text{-H})(\mu\text{-}PCy_2)(CO)_2]$ with the internal alkyne $MeO_2CC{\equiv}CCO_2Me$. The latter isomers display in each case one of the carboxylate groups *O*-bound to a Mo atom and *trans* to the phosphanyl ligand,[18] as also observed in both isomers of **3** (O–Mo–P ca. 130°). This leads to the electronic saturation of the dimetal center in these molecules, therefore to the formulation of a single intermetallic bond in both cases, in agreement with the lengths of 3.0047(5) and 2.959(3) Å observed respectively for the *cis* and *trans* isomers of **3**. The latter are only ca. 0.04 Å longer than the corresponding lengths in the mentioned carboxylate-substituted alkenyl complexes, likely reflecting the bulkier nature of the phosphanyl ligand (compared to $PCy_2$) in compounds **3**. We note that the *trans*-dicarbonyl geometry exhibited by these complexes has been structurally characterized also for the carboxylate-substituted alkenyl complexes $[W_2Cp_2(\mu\text{-}\kappa^2_{C,O}\text{:}\eta^2_{C,C}\text{-CRCHR})(\mu\text{-}PCy_2)(CO)_2]$,[19] and $[Mo_2Cp_2\{\mu\text{-}\kappa^2_{C,O}\text{:}\eta^2_{C,C}\text{-CRCHR})(\mu\text{-X})(CO)_2]$ (X= $PPh_2$, $S^iPr$; R = $CO_2Me$),[20] and for the benzoylalkenyl complex $[Mo_2Cp_2\{\mu\text{-}\kappa^2_{C,O}\text{:}\eta^2_{C,C}\text{-CHCH(C(O)Ph)}\}(\mu\text{-}PPh_2)(CO)_2]$.[21]

The geometrical parameters within the phosphanyl ligand of compounds ***cis*-3** and ***trans*-3** are comparable to those observed for the hydride complex **4**,[8,9] and deserve no comment. However, the interatomic lengths involving the bridging hydrocarbon group show some differences when compared to those measured in the alkenyl complexes mentioned above. Thus, while the bridgehead C atom displays comparable and short Mo–C lengths of ca. 2.15 Å as expected, the Mo–C length of ca. 2.35 Å for the alkenyl $\beta$-carbon is ca. 0.1 Å longer, a difference which can be identified as a steric effect derived from the presence of the bulky $^t$Bu group at this carbon atom. In contrast, the Mo–O length of ca. 2.15 Å is shorter than the corresponding lengths in the mentioned complexes (2.20-2.26 Å), thus indicating a stronger interaction, likely to balance the weaker coordination of the alkenyl $\beta$-carbon.

Spectroscopic data in solution for ***cis*-3** and ***trans*-3** are consistent with the structures found in the solid state and also comparable, when applicable, to those measured for the phosphanyl complex **4** and for the analogous isomers in the mentioned complex $[Mo_2Cp_2(\mu\text{-}\kappa^2_{C,O}\text{:}\eta^2_{C,C}\text{-CRCHR})(\mu\text{-}PCy_2)(CO)_2]$,[18] then deserving no detailed comments. The retention in solution of the solid-state structures is indicated by the IR spectra (Table 1), which display carbonyl C–O stretches with the relative intensities expected for cisoid and transoid arrangements of $M_2(CO)_2$ oscillators, respectively,[16] and by the $^{13}C\{^1H\}$ NMR spectra, which in both cases display an $\alpha$-alkenyl resonance at ca. 125 ppm strongly coupled to P ($^2J_{CP}$ 31-35 Hz), indicative of acute (cisoid) C–Mo–P coupling pathways (ca. 70° in the crystal).[22] We finally note that the formyl group is identified by characteristically deshielded resonances at ca. 8.6 ppm ($^1H$) and 165 ppm ($^{13}C$).

**The Role of High-Energy Isomers of Compound 1**. After considering the known reactivity of trigonal phosphinidene-bridged complexes of the types **A** and **B**, we may conclude that it is unlikely that compound **1** could be itself a direct precursor of compounds **2** and **3**. Thus we have searched for more reactive isomers of **1** which might be generated under photochemical conditions and account for the formation of these products. In particular, by using density functional theory (DFT) methods (see the Experimental Section), we have searched for isomers having either a pyramidal bridging ligand of type **C**, or a bent terminal phosphinidene ligand. The reason for this is that recent work on the diiron complex $[Fe_2Cp_2(PR^*)(CO)_3]$ revealed that such alternative structures were of similar energy, with the one having the bent terminal PR* group remarkably reacting with $H_2$ under mild conditions (4 atm, 293 K),[23] while possibly being also behind a C–H bond cleavage in the PR* ligand analogous to the one required to yield complexes **3**.[24] Our search on the potential energy surface of our $Mo_2$ system actually failed to find a structure with a significantly pyramidalized bridging ligand of type **C**, but we found a minimum with a terminal and significantly bent phosphinidene ligand (**1T**, Mo–P–C ca. 140°, Figure 4), having a Gibbs free energy 70 kJ/mol higher than **1**.

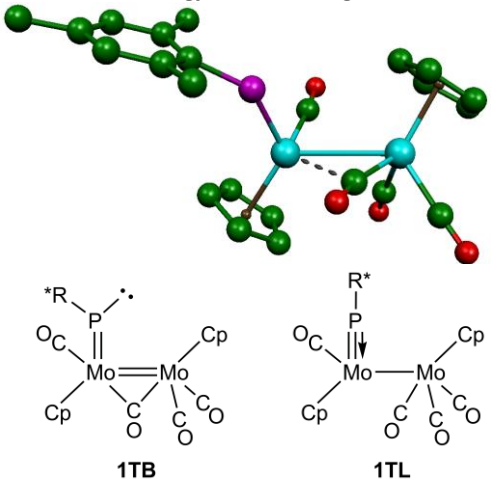


**Figure 4.** DFT-optimized structure of isomer **1T** of compound **1**, with Me groups and H atoms omitted. Selected bond lengths (Å) and angles (deg): Mo–Mo = 3.089, Mo–P = 2.212, Mo–C* = 1.997, 2.540; Mo–P–C = 142.0, Mo–C*–O = 163.4. Formal representations of the extreme structures having a fully bent (**1TB**) or linear (**1TL**) phosphinidene ligand are shown below.

Isomer **1T** has geometrical parameters actually intermediate between those expected for a molecule having a fully bent terminal ligand (**1TB**) and those for one with a linear ligand (**1TL**) (Figure 4). Thus, the intermetallic length of 3.089 Å is substantially shorter than the single-bond length in **1** (computed to be 3.307 Å, see the SI), but still a bit higher than the value of ca. 3.0 Å expected for a double Mo–Mo bond (cf. 2.960(2) Å in $[Mo_2Cp_2I_2(\mu\text{-}PR^*)(CO)_2]$),[8] and there is a carbonyl ligand involved in a semibridging (rather than bridging) interaction with the P-bearing Mo atom. In line with this, inspection of the frontier orbitals of **1T** reveals that the expected (for a bent ligand) lone-pair at the P atom is partially involved in $\pi$-bonding with the metal (as expected for a linear ligand). This mixing is represented by the HOMO–1 and HOMO–4 orbitals of **1T**, while the expected $\pi$ component of the bent ligand is represented by the HOMO–5 orbital (Figure

5). Yet the P-based nature of the HOMO–1 and LUMO orbitals should enable **1T** to induce a C–H bond cleavage,[23,25] as needed to eventually yield the phosphanyl complexes **3**. Indeed our DFT calculations indicate that **1T** (which we will represent from now on through the extreme form **1TB**) might undergo P insertion into a C–H bond in one of the *ortho*-$^t$Bu groups of the phosphinidene ligand, *via* a transition state **TS1** (Mo–Mo = 3.044 Å) placed 184 kJ/mol above **1** in tetrahydrofuran solution, to give a phosphine derivative **I1** stabilized with a four-electron-donor interaction of the bridging CO ligand (Mo–Mo= 3.322 Å, Scheme 5).[26] In the absence of any external reagent, this intermediate is expected to readily evolve *via* a P–H bond cleavage to yield the more stable hydride isomer **4** (78 kJ/mol below **1**; Mo–Mo = 3.363 Å; cf. 3.250(1) Å in the crystal) in a thermal way, because it is well known that the triply-bonded dimers $[M_2Cp_2(CO)_4]$ react with secondary phosphines $PR_2H$ under mild conditions to give the corresponding hydride derivatives $[M_2Cp_2(\mu\text{-H})(\mu\text{-}PR_2)(CO)_4]$.[27] The overall barrier for the isomerization **1**/**4** likely would be given then by **TS1**, which would be accessible in a photochemical reaction, but also thermally, in agreement with the experimental observation that **4** can be obtained photochemically, but also by refluxing a diglyme solution of **1** (ca. 438 K) for ca. 8 h.[9]

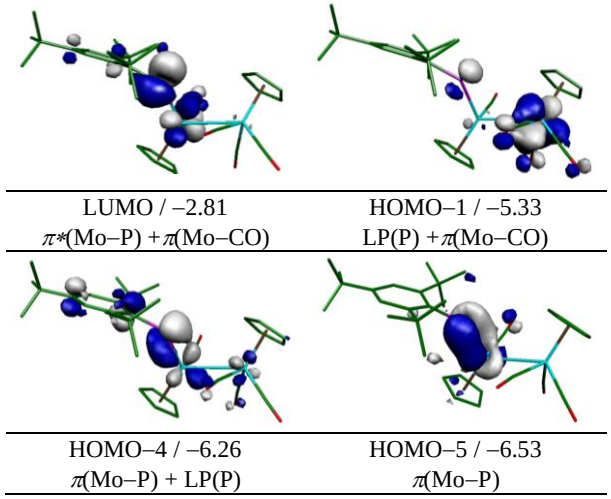


**Figure 5.** Selected molecular orbitals for isomer **1T**, with their energies (in eV) and main bonding character indicated below.

**Reaction Pathways in the Formation of Compounds 2 and 3.** The orbital and structural properties of the intermediate **1T** discussed above would enable it to react with 1-alkynes in different ways. First, **1T** could perform a nucleophilic attack to the sterically less protected terminal carbon of the alkyne thanks to the P-based nature of its HOMO–1, in a way comparable to the one proposed for pyramidal phosphinidene-bridged complexes.[5,6] This would give a zwitterionic intermediate **I2** that would easily rearrange to the final product **2** upon coordination of the alkyne carbons to the dimetal center (Scheme 6). Although we have not attempted to model this multistep transformation, which also involves a *trans* to *cis* rearrangement of the MoCp fragments, we have optimized the structure of the hypothetical complexes of type **2** having $^t$Bu and Me substituents (the latter being a close model of the isolable **2-Pr**). Interestingly, we have found that **2-Me** lies 52 kJ/mol below the starting reagents, while **2-tol** lies instead 32 kJ/mol *above* the corresponding ones. This denotes a strong thermodynamic de-stabilization effect of some 85 kJ/mol in the latter case, no doubt due to the steric repulsions induced by the bulky $^t$Bu group upon approaching the dimetal center, as required to build a complex of type **2**.

**Scheme 5. Proposed Mechanism for the Isomerization of Compound 1.**[a]

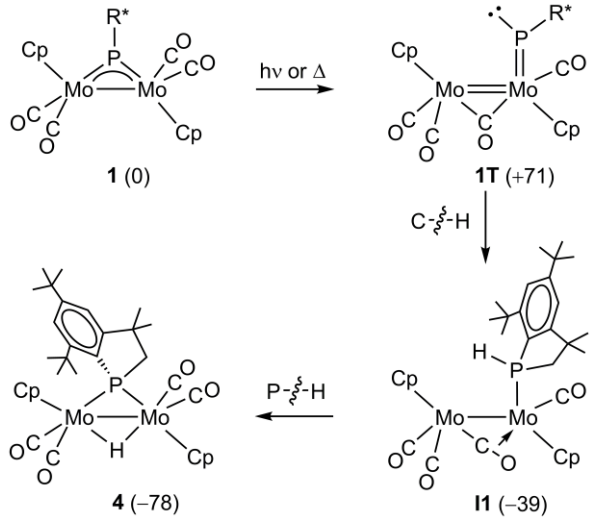


[a] Gas-phase DFT-computed Gibbs free energies (in kJ/mol at 298 K) relative to **1** indicated between brackets.

**Scheme 6. Mechanism for the Formation of Compounds 2**

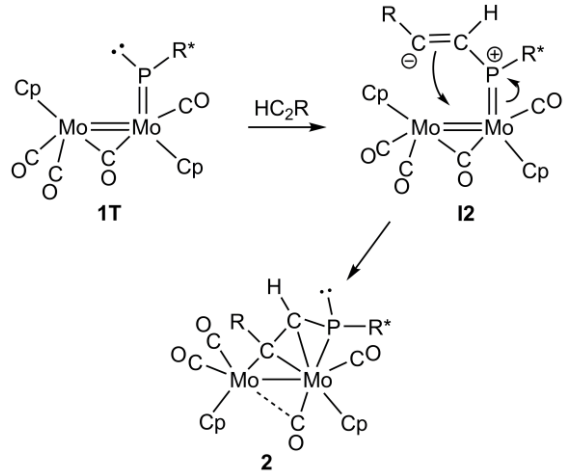


Even if **2-$^t$Bu** cannot be formed due to unbearable steric repulsions, there is no reason why some of the corresponding zwitterionic intermediate of type **I2** could not be formed, since in that case the bulky $^t$Bu group points away from the crowded dimetal center. Therefore we must assume that this initial step is a reversible one, then allowing in that case the regeneration of the phosphinidene intermediate **1T**, which might then have time to rearrange into the phosphine derivative **I1**, as discussed above. In the presence of the alkyne, however, **I1** would not rearrange into **4**, but rather would then coordinate an alkyne molecule by displacing the four-electron bridging CO into a terminal position, a well-known behavior of this sort of bridging carbonyls.[28] The ordering of elemental steps from here on is uncertain, and attempting to advance a detailed sequence would be highly speculative. Yet we can assume that, under photochemical conditions, decarbonylation might

easily follow alkyne coordination, to give the alkyne-bridged intermediate **I3** (Scheme 7). Previous work by Knox et al., and Mays et al., has shown that analogous alkyne complexes of the type $[Mo_2Cp_2(\mu\text{-}\eta^2\text{:}\eta^2\text{-}C_2R_2)(PPh_2H)(CO)_3]$ (R= H, $CO_2Me$) rearrange thermally into the corresponding formylalkenyl-bridged derivatives $[Mo_2Cp_2(\mu\text{-}PPh_2)\{\mu\text{-}\kappa^2{}_{C,O}\text{:}\eta^2{}_{C,C}\text{-}CRCRC(O)H\}(CO)_2]$, which are analogous to complexes **3**.[20,21] Therefore, we can reasonably assume that an intermediate such as **I3** (or a closely related one) would analogously rearrange readily into the final complexes of type **3**. The elemental steps needed for it are well-precedented in organometallic systems (P–H bond cleavage, carbonyl insertion into a M–H bond, and formyl/alkyne C–C coupling), but the exact sequence of elemental steps is uncertain at the moment. We note that, by performing a formyl/alkyne coupling *via* the internal carbon of the alkyne, the bulky $^t$Bu group is drawn away from the crowded dimetal center, doubtlessly a more favored event from a thermodynamic point of view.

**Scheme 7. Mechanism for the Formation of Compounds 3**

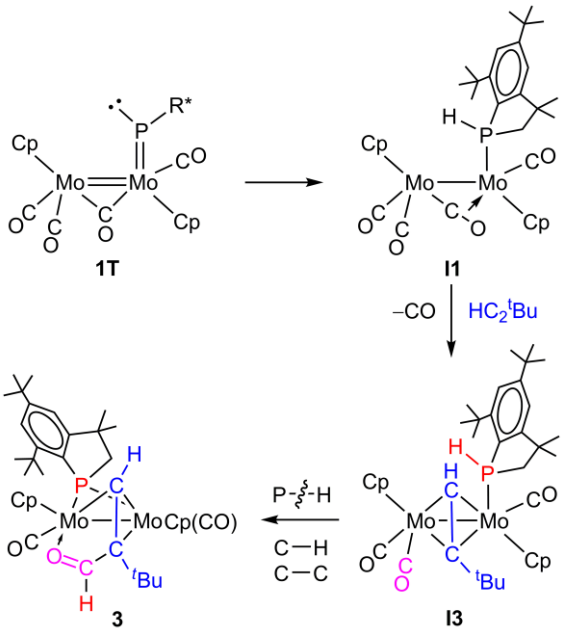


## CONCLUDING REMARKS

The divergent reactivity of the phosphinidene-bridged complex **1** toward 1-alkynes HC≡CR can be understood by considering two competitive reaction pathways of a reactive isomer **1T** having a bent terminal phosphinidene ligand (Mo–P–C ca. 140°), which is placed some 70 kJ/mol above **1** in the corresponding potential energy surface, according to DFT calculations. The faster pathway would involve the nucleophilic attack of the P atom of **1T** to the sterically more accessible terminal carbon of the alkyne, then followed by coordination of the alkyne carbons to the dimetal center, to give the phosphapropenedyil-bridged complexes **2** eventually isolated for alkynes having R groups of medium to low-size (*p*-tol, $CO_2Me$, Pr). When R is the bulky $^t$Bu group, however, this last step would lead to unbearable steric repulsions with the dimetal center, estimated in some 85 kJ/mol. Under these circumstances, isomer **1T** has time to rearrange into its phosphine isomer **I1** *via* an intramolecular C–H bond cleavage step involving one *ortho*-$^t$Bu group of the phosphinidene ligand. In the absence of additional reagents, intermediate **I1** would readily rearrange in turn *via* a P–H bond cleavage to give the phosphanyl- and hydride-bridged complex **4**, a more stable isomer (by some 80 kJ/mol) accessed through thermal or photochemical treatment of **1**. In the presence of HC≡C$^t$Bu, however, intermediate **I1** would instead add an alkyne molecule to give, after decarbonylation, an alkyne-bridged phosphine complex **I3** rapidly rearranging through a multistep pathway likely involving P–H bond cleavage, carbonyl insertion into a Mo–H bond and formyl/alkyne C–C coupling steps, to eventually yield the phosphanyl- and formylalkenyl-bridged complexes **3**.

## EXPERIMENTAL SECTION

**General Procedures and Starting Materials.** All manipulations and reactions were carried out under a nitrogen (99.995%) atmosphere using standard Schlenk techniques. Solvents were purified according to literature procedures, and distilled prior to use.[29] Compound $[Mo_2Cp_2(\mu\text{-}PR^*)(CO)_4]$ (**1**) (Cp = $\eta^5$-$C_5H_5$; R* = 2,4,6-$C_6H_2{}^tBu_3$) was prepared as described previously,[8] and all other reagents were obtained from the usual commercial suppliers and used as received, unless otherwise stated. Petroleum ether refers to that fraction distilling in the range 338-343 K. Photochemical experiments were performed using jacketed quartz or Pyrex Schlenk tubes cooled by tap water (ca. 288 K). A 400 W medium-pressure mercury lamp placed ca. 1 cm away from the Schlenk tube was used for these experiments. Chromatographic separations were carried out using jacketed columns refrigerated by tap water (ca. 288 K). Commercial aluminum oxide (activity I, 70-290 mesh) was degassed under vacuum prior to use. The latter was mixed afterwards under nitrogen with the appropriate amount of water to reach activity IV. IR stretching frequencies of CO ligands were measured in solution using $CaF_2$ windows. NMR spectra were routinely recorded at 300.13 ($^1$H), 121.50 ($^{31}$P{$^1$H}) and 75.47 MHz ($^{13}$C{$^1$H}) at 295 K in $CD_2Cl_2$ solution unless otherwise stated. Chemical shifts ($\delta$) are given in ppm, relative to internal tetramethylsilane ($^1$H, $^{13}$C) or external 85% aqueous $H_3PO_4$ ($^{31}$P). Coupling constants (*J*) are given in Hertz.

**Preparation of $[Mo_2Cp_2\{\mu\text{-}\kappa^1{}_C\text{:}\eta^3{}_{C,C,P}\text{-}C(p\text{-tol})CHPR^*\}(CO)_4]$ (2-tol)**. A THF solution (20 mL) of compound **1** (0.100 g, 0.141 mmol) and HC≡C(*p*-tol) (100 $\mu$L, 0.420 mmol) was irradiated for 25 min with visible-UV light in a quartz Schlenk tube refrigerated by tap water with a gentle $N_2$ purge, to give a brown solution. The solvent was then removed under vacuum, and the residue was dissolved in a minimum toluene (ca. 1 mL) and chromatographed on alumina at 288 K. Elution with dichloromethane/petroleum ether (3/2) gave a brown fraction yielding, after removal of solvents, compound **2-tol** as a brown microcrystalline solid (0.095 g, 81%). Anal. Calcd for $C_{41}H_{47}Mo_2O_4P$: C, 59.57; H, 5.69. Found: C, 59.69; H, 5.76. $^1$H NMR: $\delta$ 7.12 (s, 2H, $C_6H_2$), 7.03, 6.99 (AB, $^3J_{HH}$ = 8, 2 x 2H, $C_6H_4$), 5.80 (d, $^2J_{HP}$ = 2, 1H, CH), 4.77, 4.40 (2s, 2 x 5H, Cp), 2.29 (s, 3H, Me), 1.71, 1.62, 1.19 (3s, 3 x 9H, $^t$Bu). $^{13}$C{$^1$H} NMR: $\delta$ 254.4, 249.6, 241.6 (3s, MoCO), 234.5 (d, $^2J_{CP}$ = 11, MoCO), 179.1 (d, $^2J_{CP}$ = 39, $\mu$-C), 159.0, 158.8, 157.8 [3s, $C^{2,4,6}(C_6H_2)$], 148.1 [s, $C^4(C_6H_4)$], 138.7 [d, $^1J_{CP}$ = 81, $C^1(C_6H_2)$], 134.1 [s, $C^1(C_6H_4)$], 128.4 [s, $C^2(C_6H_4)$], 128.3 [s, $C^3(C_6H_4)$], 122.5, 121.0 [2s, $C^{3,5}(C_6H_2)$], 114.4 (d, $^1J_{CP}$ = 64, CH), 97.7, 94.1 (2s, Cp), 40.5, 40.2, 34.6 [3s, $C^1(^tBu)$], 36.2, 34.1, 32.0 [3s, $C^2(^tBu)$], 21.0 (s, Me).

**Preparation of $[Mo_2Cp_2\{\mu\text{-}\kappa^1{}_C\text{:}\eta^3{}_{C,C,P}\text{-}C(CO_2Me)CHPR^*\}(CO)_4]$ (2-$CO_2$Me)**. The procedure is identical to the one described for **2-tol**, but using HC≡C$CO_2$Me instead (100 $\mu$L, 1.112 mmol), to give a brown greenish solution. After similar workup, a pale green fraction was collected by elution with dichloromethane/petroleum ether (1/1) which gave, after removal of solvents, compound **2-$CO_2$Me** as a green microcrystalline solid (0.080 g, 71%). Anal. Calcd for $C_{36}H_{43}Mo_2O_6P$: C, 54.42; H, 5.45. Found: C, 54.33; H, 5.60. $^1$H NMR: $\delta$ 7.22, 7.10 (2s, 2 x 1H, $C_6H_2$), 6.16 (d, $^2J_{HP}$ = 2, 1H, CH), 5.07, 4.45 (2s, 2 x 5H, Cp), 3.69 (s, 3H, OMe), 1.67, 1.58, 1.24 (3s, 3 x 9H, $^t$Bu). $^{13}$C{$^1$H} NMR (100.63 MHz, 213 K): $\delta$ 253.7, 240.9 (2s, MoCO), 250.3 (d, $^2J_{CP}$ = 11, MoCO), 234.2 (d, $^2J_{CP}$ = 8, MoCO), 180.2 ($CO_2$Me), 157.9, 157.7, 147.8 [3s, $C^{2,4,6}(C_6H_2)$], 151.4

(d, $^2J_{CP}$ = 42, $\mu$-C), 137.6 [d, $^1J_{CP}$ = 78, C$^1$($C_6H_2$)], 129.3, 128.5 [2s, C$^{3,5}$($C_6H_2$)], 115.4 (d, $^1J_{CP}$ = 62, CH), 96.5, 93.8 (2s, Cp), 52.4 (s, OMe), 40.2, 39.6, 34.7 [3s, C$^1$($^t$Bu)], 35.9, 33.5, 30.9 [3s, C$^2$($^t$Bu)].

**Preparation of [$Mo_2Cp_2$\{$\mu$-$\kappa^1_C$:$\eta^3_{C,C,P}$-C(Pr)CHPR*\}$(CO)_4$] (2-Pr)**. The procedure is identical to the one described for **2-tol**, but using HC≡CPr instead (70 $\mu$L, 0.767 mmol), to give a brown solution. After similar workup, a brown fraction was collected by elution with dichloromethane/petroleum ether (2/3) which gave, after removal of solvents, compound **2-Pr** as a green microcrystalline solid (0.090 g, 82%). Anal. Calcd for $C_{37}H_{47}Mo_2O_4P$: C, 57.08; H, 6.08. Found: C, 56.72; H, 5.87. $^1$H NMR (400.13 MHz, 243 K): $\delta$ 7.18, 7.08 (2s, 2 x 1H, $C_6H_2$), 5.75 (s, 1H, CH), 5.36, 4.57 (2s, 2 x 5H, Cp), 2.81, 2.45 (2m, 2 x 1H, $CH_2$), 1.98, 1.80 (2m, 2 x 1H, $CH_2$), 1.64, 1.58, 1.25 (3s, 3 x 9H, $^t$Bu), 1.08 (t, $^3J_{HH}$ = 7, 3H, Me). $^{13}$C\{$^1$H\} NMR (100.63 MHz, 243 K): $\delta$ 248.8 (s, MoCO), 248.7 (m, MoCO), 241.4 (d, $^2J_{CP}$ = 6, MoCO), 238.2 (d, $^2J_{CP}$ = 20, MoCO), 197.4 (d, $^2J_{CP}$ = 34, $\mu$-C), 158.5 [d, $J_{CP}$ = 9, C($C_6H_2$)], 157.6, 147.7 [2s, C($C_6H_2$)], 138.8 [d, $^1J_{CP}$ = 80, C$^1$($C_6H_2$)], 122.6, 120.3 [2s, C$^{3,5}$($C_6H_2$)], 115.8 (d, $^1J_{CP}$ = 62, CH), 96.6, 93.9 (2s, Cp), 64.5 (s, $CH_2$), 40.3, 39.6, 34.6 [3s, C$^1$($^t$Bu)], 36.0 [s, C$^2$($^t$Bu)], 33.4 [d, $^4J_{CP}$ = 9, C$^2$($^t$Bu)], 31.8 (s, $CH_2$), 31.1 [s, C$^2$($^t$Bu)], 15.1 (s, $CH_3$).

**Preparation of *cis*-[$Mo_2Cp_2$\{$\mu$-$\kappa^2_{C,O}$:$\eta^2_{C,C}$-CHC($^t$Bu)C(O)H\}\{$\mu$-P($CH_2CMe_2$)$C_6H_2{}^t$Bu$_2$\}$(CO)_2$] (*cis*-3).** A THF solution (25 mL) of compound **1** (0.070 g, 0.099 mmol) and HC≡C$^t$Bu (75 $\mu$L, 0.597 mmol) was irradiated for 25 min with visible-UV light in a quartz Schlenk tube refrigerated by tap water with a gentle $N_2$ purge, to give a dark red solution. The solvent was then removed under vacuum, and the residue was dissolved in a minimum dichloromethane (ca. 2 mL) and chromatographed on alumina at 288 K. Elution with dichloromethane/petroleum ether (2/3) gave a very minor fraction containing isomer ***trans*-3** (see below). Elution with neat dichloromethane gave a major red fraction yielding, after removal of the solvent, compound ***cis*-3** as a red microcrystalline solid (0.041 g, 54%). The crystals used in the X-ray diffraction study were grown by the slow diffusion of a layer of petroleum ether into a concentrated dichloromethane solution of the complex at 253 K. Anal. Calcd for $C_{37}H_{49}Mo_2O_3P$: C, 58.12; H, 6.46. Found: C, 58.10; H, 6.53. $^1$H NMR: $\delta$ 8.44 [d, $^4J_{HH}$ = 2, 1H, C(O)H], 7.27 (dd, $^4J_{HP}$ = 4, $^4J_{HH}$ = 2, 1H, $C_6H_2$), 7.06 (d, $^4J_{HH}$ = 2, 1H, $C_6H_2$), 6.87 (dd, $^3J_{HP}$ = 13, $^4J_{HH}$ = 2, 1H, CH), 5.06, 4.69 (2d, $^3J_{HP}$ = 1.5, 2 x 5H, Cp), 3.04 (ABX, $^2J_{HH}$ = 15, $^2J_{HP}$ = 9, 1H, $CH_2$), 2.80 (ABX, $^2J_{HH}$ = 15, $^2J_{HP}$ = 9, 1H, $CH_2$), 1.45, 1.29, 1.00 (3s, 3 x 9H, $^t$Bu), 1.43, 1.16 (2s, 2 x 3H, Me). $^{13}$C\{$^1$H\} NMR: $\delta$ 246.3 (d, $^2J_{CP}$ = 5, MoCO), 240.4 (d, $^2J_{CP}$ = 9, MoCO), 163.6 [s, C(O)H], 157.3 [d, $^1J_{CP}$ = 14, C$^1$($C_6H_2$)], 154.6 [d, $^2J_{CP}$ = 6, C($C_6H_2$)], 152.1, 139.3 [2s, C($C_6H_2$)], 128.8 (d, $^2J_{CP}$ = 31, $\mu$-CH), 122.5 [d, $^3J_{CP}$ = 7, CH($C_6H_2$)], 118.7 [d, $^3J_{CP}$ = 9, CH($C_6H_2$)], 91.6, 88.2 (2s, Cp), 88.8 (s, *C*$^t$Bu), 51.7 (d, $^1J_{CP}$ = 27, $CH_2$), 41.7 (s, *C*$Me_2$), 38.4, 35.0, 34.8 [3s, C$^1$($^t$Bu)], 36.5 (s, Me), 32.3, 31.5, 31.1 [3s, C$^2$($^t$Bu)], 31.8 (d, $^3J_{CP}$ = 3, Me).

**Preparation of *trans*-[$Mo_2Cp_2$\{$\mu$-$\kappa^2_{C,O}$:$\eta^2_{C,C}$-CHC($^t$Bu)C(O)H\}\{$\mu$-P($CH_2CMe_2$)$C_6H_2{}^t$Bu$_2$\}$(CO)_2$] (*trans*-3).** The procedure is analogous to the one described for isomer ***cis*-3**, but now using a Pyrex Schlenk tube and a reaction time of 30 min, to give a red solution. The solvent was then removed under vacuum, and the residue was dissolved in a minimum dichloromethane (ca. 2 mL) and chromatographed on alumina at 288 K. Elution with dichloromethane/petroleum ether (2/3) gave a major orange fraction yielding, after removal of solvents, compound ***trans*-3** as an orange microcrystalline solid (0.027 g, 36%). Elution with neat dichloromethane gave a minor red fraction yielding analogously compound ***cis*-3** as a red microcrystalline solid (0.017 g, 22%). The crystals of ***trans*-3** used in the X-ray diffraction study were grown by the slow diffusion of a layer of petroleum ether into a concentrated dichloromethane solution of the complex at 253 K. Data for ***trans*-3**: Anal. Calcd for $C_{37}H_{49}Mo_2O_3P$: C, 58.12; H, 6.46. Found: C, 58.23; H, 6.58. $^1$H NMR: $\delta$ 8.79 [d, $^4J_{HH}$ = 2, 1H, C(O)H], 7.37 (dd, $^4J_{HP}$ = 4.5, $^4J_{HH}$ = 2, 1H, $C_6H_2$), 7.09 (d, $^4J_{HH}$ = 2, 1H, $C_6H_2$), 5.96 (dd, $^3J_{HP}$ = 9, $^4J_{HH}$ = 2, 1H, CH), 5.20, 4.85 (2d, $^3J_{HP}$ = 1.5, 2 x 5H, Cp), 2.62 (ABX, $^2J_{HH}$ = 13, $^2J_{HP}$ = 2, 1H, $CH_2$), 2.30 (ABX, $^2J_{HH}$ = $^2J_{HP}$ = 13, 1H, $CH_2$), 1.44 (s, 3H, Me), 1.42, 1.30, 1.05 (3s, 3 x 9H, $^t$Bu), 1.33 (d, $^4J_{HP}$ = 1, 3H, Me). $^{13}$C\{$^1$H\} NMR: $\delta$ 244.6 (d, $^2J_{CP}$ = 6, MoCO), 239.0 (d, $^2J_{CP}$ = 8, MoCO), 171.3 [s, C(O)H], 157.2 [d, $^1J_{CP}$ = 13, C$^1$($C_6H_2$)], 152.3 [d, $^4J_{CP}$ = 2, C$^4$($C_6H_2$)], 151.5 [d, $^2J_{CP}$ = 5, C$^{2,6}$($C_6H_2$)], 137.8 [d, $^2J_{CP}$ = 4, C$^{2,6}$($C_6H_2$)], 125.4 (d, $^2J_{CP}$ = 35, $\mu$-CH), 123.6 [d, $^3J_{CP}$ = 7, CH($C_6H_2$)], 118.9 [d, $^3J_{CP}$ = 8, CH($C_6H_2$)], 97.0, 88.7 (2s, Cp), 81.8 (s, *C*$^t$Bu), 44.6 (d, $^1J_{CP}$ = 26, $CH_2$), 41.8 (s, *C*$Me_2$), 38.1, 34.8, 34.6 [3s, C$^1$($^t$Bu)], 24.7, 31.3, 31.1 [3s, C$^2$($^t$Bu)], 33.3, 28.3 (2s, Me).

**X-Ray Crystal Structure Determination for Compounds *cis*-3 and *trans*-3.** In each case, a single crystal was coated in parafin oil and mounted on a glass fiber. X-ray measurements were made by using a Bruker SMART-APEX CCD area-detector diffractometer with Mo-K$\alpha$ radiation ($\lambda$ = 0.71073 Å).[30] Intensities were integrated from several series of exposures,[31] each exposure covering 0.3° in $\omega$, and the total data set being a hemisphere. Absorption corrections were applied, based on multiple and symmetry-equivalent measurements.[32] The structures were solved by direct methods and refined by least squares on weighted $F^2$ values for all reflections.[33] In general, all non-hydrogen atoms were assigned anisotropic displacement parameters and refined without positional constraints, and all hydrogen atoms were constrained to ideal geometries and refined with fixed isotropic displacement parameters. Complex neutral-atom scattering factors were used.[34] Refinements proceeded smoothly to give the residuals shown in Table S1 (see the SI). For compound ***trans*-3**, hydrogen atoms H(4) and H(6) were located in the electron density difference map, assigned isotropic displacement parameters and refined without positional constraints. For this compound, the data set was 84% complete, due to the fact that data were collected by assuming an orthorhombic space group, and COSMO was used to calculate a strategy that would collect enough reflections for orthorhombic. However, final inspection of the data revealed that the correct space group was a monoclinic one.

**Computational Details.** All DFT computations were carried out using the GAUSSIAN03 package,[35] in which the hybrid method B3LYP was used with the Becke three-parameter exchange functional[36] and the Lee−Yang−Parr correlation functional.[37] An accurate numerical integration grid (99, 590) was used for all the calculations via the keyword Int=Ultrafine. Effective core potentials and their associated double-ζ LANL2DZ basis set were used for the metal atoms.[38] The light elements (P, O, C and H) were described with the 6-31G* basis.[39] Geometry optimizations were performed under no symmetry restrictions, using initial coordinates derived from X-ray data; for compounds where this information was not available, the initial coordinates were obtained by modification of the coordinates of similar complexes. Frequency analyses were performed to ensure that all the stationary points were either a minima (no negative frequencies) or transition states (one negative frequency). Molecular orbitals and frequencies were visualized using the Molekel program.[40]

## ASSOCIATED CONTENT

### Supporting Information

A CIF file containing full crystallographic data for compounds ***cis*-3** and ***trans*-3** (CCDC 1528539 and 1528540), a PDF file containing a table with crystallographic data for the above compounds and results of DFT calculations of different compounds and intermediates (drawings, molecular orbitals and energies), and an XYZ file including the Cartesian coordinates for all computed species. The Supporting Information is available free of charge on the ACS Publications website.

## AUTHOR INFORMATION


### Corresponding Authors

E-mail: garciavdaniel@uniovi.es (D.G.-V.), mara@uniovi.es (M.A.R.).


### Notes

The authors declare no competing financial interest.

## ACKNOWLEDGMENT

We thank the MINECO of Spain (Project CTQ2015-63726-P), and the Consejería de Educación of Asturias (Project GRUPIN14-011) for financial support, and the Universidad de Oviedo for access to computing facilities. We also thank Dr. Hayrullo Hamidov and Dr. John C. Jeffery (University of Bristol) for the crystal structure determination of compounds ***cis*-3** and ***trans*-3**, and Isabel G. Albuerne (Universidad de Oviedo) for adquisition of low-temperature NMR data of compound **2-Pr**.

## REFERENCES

(1) Dillon, K. B.; Mathey, F.; Nixon, J. F. *Phosphorus: The Carbon Copy*; Wiley: New York, 1998.

(2) (a) Mathey, F.; Duan, Z. *Dalton Trans.* **2016**, *45*, 1804-1809. (b) Mathey, F. *Dalton Trans.* **2007**, 1861-1868. (c) Mathey, F.; Tran Huy, N. H.; Marinetti, A. *Helv. Chim. Acta* **2001**, *84*, 2938-2957.

(3) (a) Aktas, H.; Slootweg, J. C.; Lammertsma, K. *Angew. Chem. Int. Ed.* **2010**, *49*, 2102-2113. (b) Lammertsma, K. *Top. Curr. Chem.* **2003**, *229*, 95-119. (c) Stephan, D. W. *Angew. Chem. Int. Ed.* **2000**, *39*, 314–329.

(4) García, M. E.; García-Vivó, D.; Ramos, A.; Ruiz, M. A. *Coord. Chem. Rev.* **2017**, *330*, 1-36.

(5) (a) Alvarez, M. A.; García, M. E.; González, R.; Ruiz, M. A. *Organometallics* **2013**, *32*, 4601-4611. (b) Alvarez, M. A.; García, M. E.; González, R.; Ruiz, M. A. *Organometallics* **2008**, *27*, 1037-1040.

(6) (a) Alvarez, M. A.; Amor, I.; García, M. E.; García-Vivó, D.; Ruiz, M. A.; Suárez, J. *Organometallics* **2012**, *31*, 2749-2763. (b) Alvarez, M. A.; García, M. E.; Ruiz, M. A.; Suárez, J. *Angew. Chem. Int. Ed.* **2011**, *50*, 6383-6387.

(7) Lang, H.; Zsolnai, L.; Huttner, G. *Chem. Ber.* **1985**, *118*, 4426-4432.

(8) García, M. E.; Riera, V.; Ruiz, M. A.; Sáez, D.; Vaissermann, J.; Jeffery, J. C. *J. Am. Chem. Soc.* **2002**, *124*, 14304-14305.

(9) Amor, I.; García, M. E.; Ruiz, M. A.; Sáez, D.; Hamidov, H.; Jeffery, J. C. *Organometallics* **2006**, *25*, 4857-4869.

(10) (a) Van Gastel, F.; Carty, A. J.; Pellinghelli, M. A.; Tiripicchio, A.; Sappa, E. *J. Organomet. Chem.* **1990**, *385*, C50-C54. (b) Knoll, K.; Huttner, G.; Zsolnai. L. *J. Organomet. Chem.* **1987**, *332*, 175-199. (c) Knoll, K.; Huttner, G.; Fassler, T.; Zsolnai. L. *J. Organomet. Chem.* **1987**, *327*, 255-267. (d) Knoll, K.; Huttner, G.; Zsolnai. L. *J. Organomet. Chem.* **1986**, *312*, C57-C60. (e) Knoll, K.; Orama, O.; Huttner, G. *Angew. Chem., Int. Ed. Engl.* 1**984**, *23*, 976-977.

(11) (a) Ang, H. G.; Ang, S. G.; Du, S. *Dalton Trans.* **1999**, 2963-2970. (b) Pereira, R. M. S.; Fujiwara, F. Y.; Vargas, M. D.; Braga, D.; Grepioni, F. *Organometallics* **1997**, *16*, 4833-4838. (c) Corrigan, J. F.; Doherty, S.; Taylor, N. J.; Carty, A. J. *Organometallics* **1993**, *12*, 1365-1377. (d) Corrigan, J. F.; Doherty, S.; Taylor, N. J.; Carty, A. J. *Organometallics* **1992**, *11*, 3160-3163. (e) Jaeger, J. T.; Powell, A. K.; Vahrenkamp, H. *Chem. Ber.* **1988**, *121*, 1729-1738. (f) Lunniss, J.; MacLaughlin, S. A.; Taylor, N. J.; Carty, A. J.; Sappa, E. *Organometallics* **1985**, *4*, 2066-2068.

(12) Cordero, B.; Gómez, V.; Platero-Prats, A. E.; Revés, M.; Echevarría, J.; Cremades, E.; Barragán, F.; Alvarez, S. *Dalton Trans.* **2008**, 2832-2838.

(13) Pyykkö, P.; Atsumi, M. *Chem. Eur. J.* **2009**, *15*, 12770-12779.

(14) Arif, A. M.; Cowley, A. H.; Norman, N. C.; Orpen, A. G.; Pakulski, M. *Organometallics* **1988**, *7*, 309-318.

(15) (a) Klingler, R. J.; Butler, W. M.; Curtis, M. D. *J. Am. Chem. Soc.* **1978**, *100*, 5034-5039. (b) Crabtree, R. H.; Lavin, M. *Inorg. Chem.* **1986**, *25*, 805-812. (c) Parmelee, S. R.; Mankad, N. P. *Dalton Trans.* **2015**, *44*, 17007-17014.

(16) Braterman, P. S. *Metal Carbonyl Spectra*; Academic Press: London, U. K., 1975.

(17) Malisch, W.; Maisch, R.; Colquhoun, I. J.; McFarlane, W. *J. Organomet. Chem.* **1981**, *220*, C1-C6.

(18) Alvarez, M. A.; García, M. E.; Ramos, A.; Ruiz, M. A.; Lanfranchi, M.; Tiripicchio, A. *Organometallics* **2007**, *26*, 5454-5467.

(19) Alvarez, M. A.; García, M. E.; García-Vivó, D.; Ruiz, M. A.; Vega, M. F. *Dalton Trans.* **2016**, *45*, 5274-5289.

(20) Adams, H.; Biebricher, A.; Gay, S. R.; Hamilton, T.; McHugh, P. E.; Morris, M. J.; Mays, M. J. *J. Chem. Soc., Dalton Trans.* **2000**, 2983-2989.

(21) Doel, G. R.; Feasey, N. D.; Knox, S. A. R.; Orpen, A. G.; Webster, J. *J. Chem. Soc., Chem. Commun.* **1986**, 542-544.

(22) Jameson, C. J. in *Phosphorus-31 NMR Spectroscopy in Stereochemical Analysis*; Verkade, J. G., Quin, L. D., Eds.; VCH: Deerfield Beach, FL, 1987; Chapter 6.

(23) (a) Alvarez, M. A.; García, M. E.; García-Vivó, D.; Ramos, A.; Ruiz, M. A. *Inorg. Chem.* **2012**, *51*, 3698-3706. (b) Alvarez, M. A.; García, M. E.; González, R.; Ramos, A.; Ruiz, M. A. *Organometallics* **2010**, *29*, 1875-1878.

(24) Alvarez, M. A.; García, M. E.; González, R.; Ramos, A.; Ruiz, M. A. *Organometallics* **2011**, *30*, 1102-1115.

(25) (a) Power, P. P. *Acc. Chem. Res.* **2011**, *44*, 627-637. (b) Power, P. P. *Nature* **2010**, *463*, 171-177.

(26) Because of the low symmetry of the system, the insertion of P in the other *ortho*-$^t$Bu group takes place *via* a slightly different, a bit more energetic transition state **TS1b** placed 203 kJ/mol above **1** in tetrahydrofuran solution, which in turn leads to an isomeric phosphine derivative **I1b** which is 36 kJ/mol more stable than **1** (see the SI).

(27) (a) García, M. E.; Riera, V.; Ruiz, M. A.; Rueda, M. T.; Sáez, D. *Organometallics* **2002**, *21*, 5515-5525. (b) Woodward, S.; Curtis, M. D. *J. Organomet. Chem.* **1992**, *439*, 319-325. (c) Ebsworth, E. A. V.; Mcintosh, A. P.; Schröder, M. *J. Organomet. Chem.* **1986**, *312*, C41-C43.

(28) Liu, X. Y.; Riera, V.; Ruiz, M. A.; Bois, C. *Organometallics* **2001**, *20*, 3007-3016, and references therein.

(29) Armarego, W. L. F.; Chai, C. *Purification of Laboratory Chemicals, 7th ed.*; Butterworth-Heinemann: Oxford, UK, 2012.

(30) *SMART diffractometer control software*; Bruker Analytical X-ray Instruments Inc.: Madison, WI, 1998.

(31) *SAINT integration software*; Siemens Analytical X-ray Instruments Inc.: Madison, WI, 1994.

(32) Sheldrick, G. M. *SADABS: A program for absorption correction with the Siemens SMART system*; University of Göttingen: Göttingen, Germany, 1996.

(33) *SHELXTL program system version 5.1;* Bruker Analytical X-ray Instruments Inc.: Madison, WI, 1998.

(34) *International Tables for Crystallography;* Kluwer: Dordrecht, The Netherlands, 1992, vol. C.

(35) *Gaussian 03, Revision B.02*, Frisch, M. J.; Trucks, G. W.; Schlegel, H. B.; Scuseria, G. E.; Robb, M. A.; Cheeseman, J. R.; Montgomery, Jr., J. A.; Vreven, T.; Kudin, K. N.; Burant, J. C.; Millam, J. M.; Iyengar, S. S.; Tomasi, J.; Barone, V.; Mennucci, B.; Cossi, M.; Scalmani, G.; Rega, N.; Petersson, G. A.; Nakatsuji, H.; Hada, M.; Ehara, M.; Toyota, K.; Fukuda, R.; Hasegawa, J.; Ishida, M.; Nakajima, T.; Honda, Y.; Kitao, O.; Nakai, H.; Klene, M.; Li, X.; Knox, J. E.; Hratchian, H. P.; Cross, J. B.; Bakken, V.; Adamo, C.; Jaramillo, J.; Gomperts, R.; Stratmann, R. E.; Yazyev, O.; Austin, A. J.; Cammi, R.; Pomelli, C.; Ochterski, J. W.; Ayala, P. Y.; Morokuma, K.; Voth, G. A.; Salvador, P.; Dannenberg, J. J.; Zakrzewski, V. G.; Dapprich, S.; Daniels, A. D.; Strain, M. C.; Farkas, O.; Malick, D. K.; Rabuck, A. D.; Raghavachari, K.; Foresman, J. B.; Ortiz, J. V.; Cui, Q.; Baboul, A. G.; Clifford, S.; Cioslowski, J.; Stefanov, B. B.; Liu, G.; Liashenko, A.; Piskorz, P.; Komaromi, I.; Martin, R. L.; Fox, D. J.; Keith, T.; Al-Laham, M. A.; Peng, C. Y.; Nanayakkara, A.; Challacombe, M.; Gill, P. M. W.; Johnson, B.; Chen, W.; Wong, M. W.; Gonzalez, C.; and Pople, J. A.; Gaussian, Inc., Wallingford CT, 2004.

(36) Becke, A. D. *J. Chem. Phys.* **1993**, *98*, 5648-5652.

(37) Lee, C.; Yang, W.; Parr, R. G. *Phys. Rev. B* **1988**, *37*, 785-789.

(38) Hay, P. J.; Wadt, W. R. *J. Chem. Phys.* **1985**, *82*, 299-310.

(39) (a) Hariharan, P. C.; Pople, J. A. *Theor. Chim. Acta* **1973**, *28*, 213-222. (b) Petersson, G. A.; Al-Laham, M. A. *J. Chem. Phys.* **1991**, *94*, 6081-6090. (c) Petersson, G. A.; Bennett, A.; Tensfeldt, T. G.; Al-Laham, M. A.; Shirley, W. A.; Mantzaris, J. *J. Chem. Phys.* **1988**, *89*, 2193-2218.

(40) Portmann, S.; Luthi, H. P. *Chimia* **2000**, *54*, 766-770.

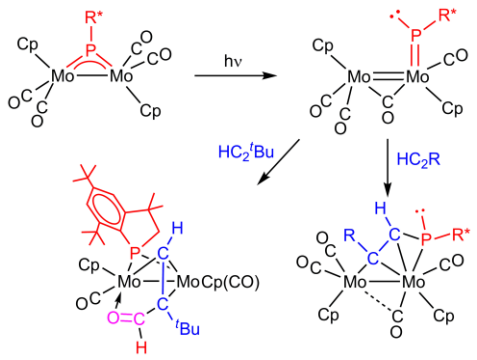


Table of Contents artwork